

This discussion paper is/has been under review for the journal Biogeosciences (BG).
Please refer to the corresponding final paper in BG if available.

Regional differences in modelled net production and shallow remineralization in the North Atlantic subtropical Gyre

B. Fernández-Castro¹, L. Anderson², E. Marañón¹, S. Neuer³, B. Ausín¹, M. González-Dávila⁴, J. M. Santana-Casiano⁴, A. Cianca⁴, R. Santana⁴, O. Llinás⁵, M. J. Rueda⁶, and B. Mourinho-Carballido¹

¹Departamento de Ecoloxía e Bioloxía Animal, Universidade de Vigo, Vigo, Pontevedra, 36200, Spain

²Applied Ocean Physics and Engineering Department, Woods Hole Oceanographic Institution, Woods Hole, MA 02543-1541, USA

³School of Life Sciences, Arizona State University, Tempe, AZ 85287-4501, USA

⁴Universidad de Las Palmas de Gran Canaria (ULPGC), Campus Universitario de Tafira s/n. 35017 Las Palmas de Gran Canaria, Spain

⁵Plataforma Oceánica de Canarias (PLOCAN), Crta. de Taliarte s/n, P.O. Box 413, 35200 Telde, Gran Canaria, Spain

Regional differences in NP and shallow remineralization

B. Fernández-Castro et al.

Title Page

Abstract

Introduction

Conclusions

References

Tables

Figures



Back

Close

Full Screen / Esc

Printer-friendly Version

Interactive Discussion



⁶Instituto Canario de Ciencias Marinas, Gobierno de Canarias, Telde, Gran Canaria, Spain

Received: 5 December 2011 – Accepted: 7 December 2011 – Published: 22 December 2011

Correspondence to: B. Fernández-Castro (bieito.fernandez@uvigo.es)

Published by Copernicus Publications on behalf of the European Geosciences Union.

BGD

8, 12477–12519, 2011

**Regional differences
in NP and shallow
remineralization**

B. Fernández-Castro et
al.

Title Page

Abstract

Introduction

Conclusions

References

Tables

Figures

⏪

⏩

◀

▶

Back

Close

Full Screen / Esc

Printer-friendly Version

Interactive Discussion



Abstract

We used 5-year concomitant data of tracers distribution from the BATS (Bermuda Time-series Study) and ESTOC (European Station for Time-Series in the Ocean, Canary Islands) sites to build a 1-D tracer model conservation including horizontal advection and compute net production and shallow remineralization rates at both sites. Net production rates computed below the mixed layer to 110 m from April to December for oxygen, dissolved inorganic carbon and nitrate at BATS ($1.34 \pm 0.79 \text{ mol O}_2 \text{ m}^{-2}$, $-1.73 \pm 0.52 \text{ mol C m}^{-2}$ and $-125 \pm 36 \text{ mmol N m}^{-2}$) showed no statistically significant differences compared to ESTOC ($1.03 \pm 0.62 \text{ mol O}_2 \text{ m}^{-2}$, $-1.42 \pm 0.30 \text{ mol C m}^{-2}$ and $-213 \pm 56 \text{ mmol N m}^{-2}$). Shallow remineralization rates between 110 and 250 m computed at ESTOC ($-3.9 \pm 1.0 \text{ mol O}_2 \text{ m}^{-2}$, $1.53 \pm 0.43 \text{ mol C m}^{-2}$ and $38 \pm 155 \text{ mmol N m}^{-2}$) were statistically higher for oxygen compared to BATS ($-1.81 \pm 0.37 \text{ mol O}_2 \text{ m}^{-2}$, $1.52 \pm 0.30 \text{ mol C m}^{-2}$ and $147 \pm 43 \text{ mmol N m}^{-2}$). Lateral advection, which was more significant at ESTOC, was responsible for the differences in estimated oxygen remineralization rates between both stations. Due to the relevance of the horizontal transport at ESTOC, we cannot assert that the differences in shallow remineralization rates computed for both stations can explain the observed discrepancies in the flux of sinking organic matter.

1 Introduction

The ocean is responsible for an annual photosynthetic fixation of $\sim 50 \text{ Pg}$ of carbon which represents around half of the global primary production (Field et al., 1998). Carbon fixation by marine phytoplankton and its transport to the deep ocean, known as the biological carbon pump, plays a key role in the ocean-atmosphere CO_2 exchange, and hence affects climate in time-scales from decades to thousands of years. The carbon pump efficiency is not constant and depends on several factors such as the input of nutrients into the euphotic layer, the balance between synthesis and remineralization of organic matter or the planktonic community composition.

Regional differences in NP and shallow remineralization

B. Fernández-Castro et al.

Title Page

Abstract

Introduction

Conclusions

References

Tables

Figures

◀

▶

◀

▶

Back

Close

Full Screen / Esc

Printer-friendly Version

Interactive Discussion



**Regional differences
in NP and shallow
reminerzalization**

B. Fernández-Castro et
al.

[Title Page](#)[Abstract](#)[Introduction](#)[Conclusions](#)[References](#)[Tables](#)[Figures](#)[Back](#)[Close](#)[Full Screen / Esc](#)[Printer-friendly Version](#)[Interactive Discussion](#)

Subtropical gyres represent the central part of the ocean and are characterized by a strong stratification of the water column. This translates into a weak input of nutrients into the euphotic layer and, as a consequence, low phytoplankton biomass and productivity. Because of their oligotrophic characteristics they have been traditionally considered oceanic deserts. However, from the point of view of carbon export from the euphotic zone, subtropical gyres were found to be surprisingly productive (Emerson et al., 1997). This fact, combined with their vast extension (~60% of the total ocean surface), results in their contribution of at least 30% of total marine new production (Najjar and Keeling, 2000).

The North Atlantic subtropical gyre (NASG) is one of the best studied open ocean regions, and in the past decades, it has been a major contributor to the development of our understanding of biogeochemical cycles in subtropical regions. Traditionally subtropical gyres have been considered relatively constant ecosystems in time and space. However, the comparative study of time-series data revealed that spatial heterogeneity is important in understanding the biogeochemistry of this biome (Neuer et al., 2002a; Mouriño-Carballido and Neuer, 2008). Two time-series stations, BATS (Bermuda Atlantic Time-series Study, 31.7° N–64.2° W) and ESTOC (European Station for Time series in the Ocean, Canary Islands, 29.16° N–15.5° W), are located at about the same latitude in the western (NASW) and eastern (NASE) portions of NASG. The monthly sampling program was initiated in October 1988 at BATS and in February 1994 at ESTOC, with the aim of tracking seasonal, inter-annual and inter-decadal changes in several biogeochemical variables (Steinberg et al., 2001; Neuer et al., 2007). Although both stations exhibit typical oligotrophic characteristics, they are characterized by different hydrographic dynamics. BATS is located in the recirculation of the Gulf Stream and it is strongly affected by mesoscale activity (Cianca et al., 2007). ESTOC is entrained by the Canary Current and is indirectly influenced by the coastal African upwelling, which export nutrients and organic matter towards the center of the gyre by means of upwelling filaments and Ekman transport (Pelegrí et al., 2005; Álvarez-Salgado et al., 2007). It is important to note that upwelling filaments do not influence ESTOC directly

(Davenport et al., 2002), and this station is considered oligotrophic based on nutrient scarcity and phytoplankton biomass and production rates (Neuer et al., 2007).

Although both stations are characterized by similar phytoplankton biomass and primary production rates, annual mean carbon export measured by using sediment traps is significantly lower at ESTOC, by a factor of 3–5, than at BATS (Neuer et al., 2002a; Helmke et al., 2010). Assuming that the euphotic zone is in steady state, higher export production should be sustained by larger inputs of nutrients and/or organic matter into the euphotic zone. It has been proposed that differences in the nutrients input could be due to the more intense mesoscale activity observed at BATS (Siegel et al., 1999; Mouriño et al., 2003). A comparative study using 10-year BATS and ESTOC data combined with satellite altimetry data indicated that the higher physical forcing dominant at BATS, deeper mixed layers and more intense mesoscale dynamics, is partly compensated by the shallower nutricline observed at ESTOC (Cianca et al., 2007). According to these authors, NASE receives ~75% of the nutrients available for new production at NASW, although this difference is not statistically significant. Another source of new nitrogen that could explain the observed differences in carbon export between the two stations is biological nitrogen fixation. Recent studies indicate that this process has a significant contribution to total new nitrogen inputs in oligotrophic waters (Capone et al., 2005; Mouriño-Carballido et al., 2011; Bonnet et al., 2011). Biogeochemical estimates suggest a lower contribution of nitrogen fixation at ESTOC compared with BATS (Neuer et al., 2002a).

The differences observed between the two stations in export rates of particulate organic carbon could also be a consequence of differences in the remineralization rates of the sinking organic matter. The comparative analysis of respiration rates determined from in vitro oxygen evolution experiments conducted in the NASE and NASW indicated higher oxygen consumption rates in the eastern part (Mouriño-Carballido and Neuer, 2008). It has been shown that atmospheric dust deposition can strongly stimulate bacterial respiration (Pulido-Villena et al., 2008). A recent study demonstrated that the most frequent and intense response of the microbial plankton to atmospheric

BGD

8, 12477–12519, 2011

Regional differences in NP and shallow remineralization

B. Fernández-Castro et al.

Title Page

Abstract

Introduction

Conclusions

References

Tables

Figures

⏪

⏩

◀

▶

Back

Close

Full Screen / Esc

Printer-friendly Version

Interactive Discussion



dust deposition in the Tropical Atlantic is the stimulation of the bacterial activity rather than phytoplankton primary production (Marañón et al., 2010). This is consistent with the results found at ESTOC, which is strongly influenced by the natural atmospheric deposition of Saharan dust and, where phytoplanktonic production seems not to be affected by aerosol inputs (Neuer et al., 2004).

For the first time, concomitant data of tracers distribution from the BATS and ESTOC time-series sites were analysed and used to build up a 1-D tracer conservation diagnostic model. The model was used to compute net production and shallow remineralization rates at both sites. The main goal of this study was to verify if differences in the synthesis and consumption of organic matter could explain the lower export rates of particulate organic carbon observed at ESTOC.

2 Comparison of the seasonal cycles at BATS and ESTOC

Monthly climatologies were calculated for temperature, salinity, density anomaly (σ_T), oxygen, dissolved inorganic carbon (DIC), nitrate (actually nitrate + nitrite) and chlorophyll-*a*, using the BATS and ESTOC data collected for the period 1996–2001 (Fig. 1). BATS and ESTOC measurements were made monthly except during the spring bloom period at BATS (February–April) when biweekly samplings were conducted. Discrete data were first interpolated to a grid with the following depths: 5, 10, 20, 40, 60, 80, 100, 110, 120, 140, 160, 200 and 250 m. The seasonal cycle was then constructed by averaging data from each depth onto a temporal grid of 15 days using a weighted moving average with a normal weighting factor, f_i^n , and a window of 50 days:

$$\langle C^n \rangle = \sum_i f_i^n C_i$$
$$f_i^n = \exp \left[- \left(\frac{t^n - t_i}{\sigma} \right)^2 \right] \quad (1)$$

Regional differences in NP and shallow remineralization

B. Fernández-Castro et al.

Title Page

Abstract

Introduction

Conclusions

References

Tables

Figures

⏪

⏩

◀

▶

Back

Close

Full Screen / Esc

Printer-friendly Version

Interactive Discussion



where C is the averaged variable, t is the time of the year in days (0–365), i is the index of the discrete data point, n is the index for the temporal grid and $\sigma = 35$ days is a constant time scale. The mixed layer depth was calculated as the depth where temperature differs 0.1°C from the 10 m value.

BATS and ESTOC exhibit a similar seasonality in the hydrographic conditions characterized by a period of winter mixing from November to March followed by a period of summer stratification from May to September (Fig. 1). The maximum winter mixing occurs later (mid-March) at BATS compared to ESTOC (February). The transition between both periods is controlled by the seasonal cycle of solar irradiation and changes in the wind speed. Seasonality is more intense at BATS where surface temperature increases from a minimum of $\sim 20^\circ\text{C}$ in mid-March to a maximum of $\sim 28^\circ\text{C}$ in August. At ESTOC temperature reaches a minimum of $18\text{--}19^\circ\text{C}$ in February and a maximum of $\sim 24^\circ\text{C}$ in September. This maximum appears later than at BATS because the intensification of the Trade Winds affects the ESTOC site during the summer period. Maxima mixed layers are deeper at BATS (193 ± 26 m) than at ESTOC (146 ± 32 m). Summer stratification is also more intense at BATS, where mixed layers during this period reach ~ 20 m. Mixed layers at ESTOC extend to a depth of ~ 50 m due to the Trade Winds intensification that enhances mixing during July–August. The main difference between both stations in salinity appears during the summer, when mixed layer values are fresher at BATS due to the rain intensification.

Chlorophyll concentration is strongly influenced by the physical forcing at both stations. Phytoplankton blooms occur in late winter/spring, after the mixed layer extends below the nutricline, with greatest monthly values of chlorophyll concentration similar for both stations (ca. 0.3 mg m^{-3}). As water column stratification increases, surface chlorophyll decreases and a deep chlorophyll maximum establishes at ca. 100 m at BATS and ESTOC. This biological activity as well as the physical forcing determine the concentration of the chemical tracers considered in this study.

The oxygen seasonal cycle in the mixed layer at both stations is characterized by maximum values during the winter period due to the increase in solubility. The

**Regional differences
in NP and shallow
remineralization**B. Fernández-Castro et
al.

Title Page

Abstract

Introduction

Conclusions

References

Tables

Figures

◀

▶

◀

▶

Back

Close

Full Screen / Esc

Printer-friendly Version

Interactive Discussion



**Regional differences
in NP and shallow
remineralization**B. Fernández-Castro et
al.

Title Page

Abstract

Introduction

Conclusions

References

Tables

Figures

⏪

⏩

◀

▶

Back

Close

Full Screen / Esc

Printer-friendly Version

Interactive Discussion



temperature increase during the summer months causes a drop in solubility and hence in surface oxygen concentration. As stratification increases during summer, oxygen accumulates below the mixed layer (~ 40 m at BATS and ~ 60 m at ESTOC). This accumulation is clearly pictured by the oxygen anomaly distribution that represents the excess of oxygen concentration above the solubility equilibrium. The oxygen anomaly distribution shows that whereas the photic layer (ca. 100 m at both sites, Cianca et al. (2007)) at ESTOC is oversaturated during the whole year, at BATS is undersaturated during the winter period. This difference is probably due to the different intensity in the mixing and ventilation of deep waters that characterizes both stations. The seasonal variability in the oxygen cycle is also weaker at ESTOC, where the maximum amplitude of the accumulation in oxygen anomaly below the mixed layer was ~ 9 mmol m^{-3} (from February to August), versus ~ 17 mmol m^{-3} (from February to September) at BATS. The oxygen anomaly distribution in the euphotic zone has a mirror-like image below this layer. Oxygen concentration increases during winter-spring as a result of the mixing with oxygen-rich surface waters and it is maximum in April–May. Then, during summer stratification oxygen concentration decreases, being the minimum values at 200 m observed in January (BATS) and November (ESTOC). Despite the differences observed in the euphotic zone, the maximum amplitude of the oxygen signal at 200 m (~ 7 mmol m^{-3}) is similar in both stations.

DIC concentrations in the mixed layer are greatest in April (BATS) and March (ESTOC), due to mixing with deeper waters and, to a lesser extend, to air-sea exchange (Marchal et al., 1996; Gruber et al., 1998; González-Dávila et al., 2003). Surface DIC concentrations decline to minimum values in October, this decline is more pronounced at BATS (~ 44 mmol m^{-3}) compared to ESTOC (~ 15 mmol m^{-3}). Below the euphotic zone DIC accumulation occurs in concert with to the observed oxygen decline. The DIC accumulation at 200 m from April to January (BATS) and from April to October (ESTOC) is 6 mmol m^{-3} and 8.7 mmol m^{-3} , respectively.

Nitrate concentration is very low in the euphotic zone at both stations. The nitracline (> 0.5 mmol m^{-3}) is generally shallower at ESTOC (90.3 ± 5.0 m) compared to

BATS (104 ± 14 m) but with a greater vertical variability at the western station. As a consequence of the influence of the nutrient poor 18°C Subtropical Mode Water at BATS, nitrate concentration below the nitracline is higher at ESTOC. Below the euphotic zone nitrate accumulates from June to January at BATS and from May to December at ESTOC, the amplitude of the accumulation at 200 m is very similar in both stations (0.7 mmol m^{-3}).

The seasonal variability of the tracers considered in this study, in agreement with previous reports (Menzel and Ryther, 1959; Jenkins and Goldman, 1985; Marchal et al., 1996; González-Dávila et al., 2003; Neuer et al., 2007; Santana-Casiano et al., 2007), is consistent with the fact that synthesis of organic matter occurs in the euphotic layer and that this matter is remineralized, at least partially, in the shallow aphotic zone between 100–250 m. In order to quantify the contribution of the biological processes and the physical forcing to the observed seasonal variability of the chemical tracers, a 1-D diagnostic model was implemented.

3 Model implementation

3.1 Model general description

We adapted the tracer conservation model based on Ono et al. (2001), who estimated the shallow remineralization at BATS for the period 1992–1998. This approach includes the main physical processes that occur below the mixed layer when convective winter mixing is not the dominant process. These processes are vertical diffusion, vertical advection (Ekman transport) and lateral advection. The used tracer conservation equation was

$$\frac{\partial C}{\partial t} = -u \frac{\partial C}{\partial x} - v \frac{\partial C}{\partial y} - w \frac{\partial C}{\partial z} + \frac{\partial}{\partial z} \left(K \frac{\partial C}{\partial z} \right) + J_C \quad (2)$$

where $C = C(t, z)$ represents temperature (T) or the tracer (oxygen, DIC, nitrate) concentration for each depth, z , and time t ; $u(t, z)$ and $v(t, z)$ are the longitudinal and

BGD

8, 12477–12519, 2011

Regional differences in NP and shallow remineralization

B. Fernández-Castro et al.

Title Page

Abstract

Introduction

Conclusions

References

Tables

Figures

⏪

⏩

◀

▶

Back

Close

Full Screen / Esc

Printer-friendly Version

Interactive Discussion



3.2 Model inputs

3.2.1 Horizontal advection

Horizontal gradients of temperature, oxygen and nitrate were calculated using the four grid points surrounding BATS and ESTOC at the World Ocean Atlas 2009 monthly climatology (WOA09) (Locarnini et al., 2010; Garcia et al., 2010b,a). Longitudinal and latitudinal gradients were computed using averaged values for each x and y components. DIC data for the same locations were obtained from the Global Distribution of Total Inorganic Carbon and Total Alkalinity Below the Deepest Winter Mixed Layer Depths climatology (Goyet et al., 2000), which includes lower temporal resolution tri-monthly averaged data.

Horizontal velocities, u and v , were assumed to be geostrophic and computed from the monthly temperature and salinity WOA09 data (Locarnini et al., 2010; Antonov et al., 2010) and the thermal wind equations. Water density was calculated using the Millero and Poisson (1981) parametrization. The thermal wind equations were integrated down to 3000 m, which was assumed as the level of no motion following Siegel and Deuser (1997). The calculated geostrophic flow for BATS ($0.02\text{--}0.04\text{ m s}^{-1}$) was directed southwest during the whole year (see Fig. 2), consistent with the fact that BATS is influenced by the Gulf Stream recirculation (Siegel and Deuser, 1997; Ono et al., 2001). The flow intensity was more variable near ESTOC ($0.02\text{--}0.07\text{ m s}^{-1}$), where the current was directed southwest during most of the year except between March and April, when u was eastward, and during the transition from spring to summer (May–July) when v was northward. This pattern is consistent with the results described by Neuer et al. (2007) and Pelegrí et al. (2005).

Due to the implementation imposed to ensure volume conservation (see next section), lateral transport included a non-geostrophic component. Further on we will use geostrophic horizontal advection to refer to the geostrophic component of the lateral transport and horizontal advection to refer to the total corrected lateral transport.

BGD

8, 12477–12519, 2011

Regional differences in NP and shallow remineralization

B. Fernández-Castro et al.

Title Page

Abstract

Introduction

Conclusions

References

Tables

Figures

◀

▶

◀

▶

Back

Close

Full Screen / Esc

Printer-friendly Version

Interactive Discussion

Additionally, model runs where the geostrophic transport term was set to zero ($u = v = 0$) were used to determine the influence of the geostrophic transport in the computed biological rates.

3.2.2 Vertical advection

Ekman downwelling/upwelling velocity, w , was computed for both stations from the wind stress monthly climatological data included in the International Comprehensive Ocean-Atmosphere Data Set, with a spatial resolution of $2^\circ \times 2^\circ$ (Leetmaa and Bunker, 1978). The computed Ekman velocity at BATS was negative during most of the year and characterized by a clear seasonal cycle (see Fig. 3a). Downwelling was maximum in February (-96 m yr^{-1}) and minimum in September, when a weak upwelling was computed (10 m yr^{-1}). These results are in agreement with the harmonic function used by Musgrave et al. (1988) and Ono et al. (2001) at BATS. The Ekman velocity was lower at ESTOC where the seasonal cycle was characterized by relatively weak upwelling during the summer (ca. 20 m yr^{-1}) and relatively weak downwelling during the rest of the year.

The Ekman velocity was set to zero at the surface and increased linearly to the Ekman depth, which was considered as the minimum value of 30 m and the mixed layer depth, and decreased linearly to zero down to 250 m (Ono et al., 2001). As the depth-dependent w requires horizontal convergence or divergence for volume conservation, horizontal advection included a correction term. This was accomplished numerically by implicitly evaluating $w \partial C / \partial z$ at the grid box interfaces.

3.2.3 Shortwave solar radiation

The effect of the solar shortwave radiation that penetrates below the mixed layer (J_C term for the temperature model) was computed as:

$$J_C^T(t, z) = \frac{1}{\rho(t, z) C_\rho(t, z)} \frac{\partial I(t, z)}{\partial z}, \quad (5)$$

12488

BGD

8, 12477–12519, 2011

Regional differences in NP and shallow remineralization

B. Fernández-Castro et al.

Title Page

Abstract

Introduction

Conclusions

References

Tables

Figures

⏪

⏩

◀

▶

Back

Close

Full Screen / Esc

Printer-friendly Version

Interactive Discussion



where ρ is the water density computed from temperature and salinity seasonal cycles using the Millero and Poisson (1981) formulation, C_p is the specific heat (Fofonoff and Millard, 1983), and $I(t, z)$ is the shortwave radiation flux computed by using the attenuation model of Paulson and Simpson (1977) for Type I water and the surface shortwave radiation values (Fig. 3b). These values were obtained by fitting to an harmonic function monthly data for the period 1996–2001 obtained from the CORE.2 Global Air-Sea flux dataset close to both sites. Annual means and amplitudes of the harmonic function were $182 \pm 5 \text{ W m}^{-2}$ and $87 \pm 6 \text{ W m}^{-2}$ at BATS, and $191 \pm 5 \text{ W m}^{-2}$ and $68 \pm 8 \text{ W m}^{-2}$ at ESTOC, respectively. Surface I was minimum in January for both stations.

3.3 Temperature model and K optimization

Similar to the approach followed by Musgrave et al. (1988), Ono et al. (2001) and Mouriño-Carballido and Anderson (2009) we computed the vertical diffusivity (K) from the optimization of the simulated temperature (T) seasonal cycle (Fig. 4). An optimized value of K was obtained every 15 days by minimizing the following function for each run:

$$\text{Cost}(t) = \left(\int_{\text{MLD}(t)}^{250\text{m}} (T_{\text{obs}}(t, z) - T_{\text{mod}}(t, z))^2 dz \right)^{1/2} \quad (6)$$

The annual mean K was $2.0 \pm 1.5 \text{ cm}^2 \text{ s}^{-1}$ for BATS and $1.5 \pm 1.6 \text{ cm}^2 \text{ s}^{-1}$ for ESTOC. The maximum K at BATS was set to $5 \text{ cm}^2 \text{ s}^{-1}$ on account of numerical limitations in the biological source term calculations due to the high values computed during the winter mixing. At ESTOC higher K values were computed in July and August, possibly related to Trade Wind intensification during the summer months.

The comparison of the temperature rate of change computed from the observed and simulated seasonal cycles showed a good agreement for both stations (Fig. 5). The

BGD

8, 12477–12519, 2011

Regional differences in NP and shallow remineralization

B. Fernández-Castro et al.

Title Page

Abstract

Introduction

Conclusions

References

Tables

Figures

⏪

⏩

◀

▶

Back

Close

Full Screen / Esc

Printer-friendly Version

Interactive Discussion



errors in the simulation of the temperature seasonal cycle were computed as:

$$\text{Err}(t, z) = \text{abs} \left(\frac{T_{\text{mod}}(t, z) - T_{\text{obs}}(t, z)}{T_{\text{obs}}(t, z)} \right). \quad (7)$$

Model errors were related to a deficient parametrization of the constant vertical diffusivity especially during strong mixing events. Higher errors were computed during the periods of strong winter mixing for both stations, just below the mixed layer in June–July (BATS) and August–September (ESTOC), and between 100 and 250 m in September at BATS and June–September at ESTOC. Ono et al. (2001) used a single K optimized for the whole year, however we observed that optimizing K for each 15-day period reduced the total integrated error in the simulation of the temperature seasonal cycle by 13 % at BATS and 20 % at ESTOC (data not shown). Figure 5d shows the contribution of the geostrophic horizontal advection to the temperature rate of change. This contribution was more important at ESTOC, where an input of warmer water was computed in June–July and colder water in September.

3.4 Integrated budgets and errors estimation

Net production rates below the mixed layer were computed by integrating the biological source term (J_C) from this depth to the estimated compensation depth. This depth was set to 110 m based on the J_C distribution and the examination of rates sensitivity to this limit (see below). To compute shallow remineralization, J_C was integrated from the compensation depth down to 250 m. Both rates were integrated between April and December in order to avoid the period of intense winter mixing. The physical model terms were also integrated for the same period and depth intervals to evaluate their contribution to the change in the tracer inventories.

Uncertainties associated with the integrated budgets were estimated by using Monte Carlo simulations. A high number ($N > 100$) of model runs for all the tracers (including temperature for K optimization) were performed with each element of the model inputs being randomly generated from a Gaussian distribution. The standard deviation

BGD

8, 12477–12519, 2011

Regional differences in NP and shallow remineralization

B. Fernández-Castro et al.

Title Page

Abstract

Introduction

Conclusions

References

Tables

Figures

⏪

⏩

◀

▶

Back

Close

Full Screen / Esc

Printer-friendly Version

Interactive Discussion



temperature simulation (see Fig. 5c), and they are probably related to limitations in the diffusivity optimization. DIC consumption occurred just below the mixed layer during summer stratification. For this tracer the compensation depth was slightly shallower (ca. 60–80 m), and maximum production was computed at 120 m during the summer.

5 The distribution of J_C for nitrate was very similar to DIC but the compensation depth was located deeper (ca. 110–115 m). Maximum nitrate consumption was computed at 80 m during May–June. Maximum production occurred at 120 m coinciding with the maximum rates of DIC (oxygen) production (consumption), and slightly shallower than the maximum described by Ono et al. (2001) at 140 m. A second maximum in nitrate
10 remineralization was observed at 250 m close to the model border.

The distribution of J_C at ESTOC was in general very similar to the patterns described for BATS although a few differences were observed. The oxygen compensation depth was located deeper at ca. 115 m. Highest rates of oxygen production were also located deeper (ca. 100 m), coinciding with the deep chlorophyll maximum. The vertical structure of the spring-summer remineralization was also different compared to
15 BATS, as maxima rates instead of being located at specific depths occurred through out the whole water column. Another important difference with BATS was observed in September–November when high oxygen (DIC, nitrate) consumption (production) was computed through the whole water column. This feature coincided with significant in-
20 puts of oxygen and nitrate, and also cold water (Fig. 5d), through horizontal advection. The role of the horizontal transport in the seasonality of the synthesis and remineralization of organic matter has been previously reported in the Canary region, which is under the influence of the coastal African upwelling (Neuer et al., 2002b; Arístegui et al., 2003; Pelegrí et al., 2005; Alonso-González et al., 2009). Upwelling filaments
25 and Ekman transport export particulate and dissolved organic matter from the coastal upwelling to the open ocean. During this transport organic matter is remineralized, at least partially, providing an external source for nutrients (Pelegrí et al., 2005). According with these authors the relevance of this process is higher during the fall. These facts indicate that at ESTOC, even though removed from direct influence of the upwelling

Regional differences in NP and shallow remineralization

B. Fernández-Castro et al.

[Title Page](#)[Abstract](#)[Introduction](#)[Conclusions](#)[References](#)[Tables](#)[Figures](#)[Back](#)[Close](#)[Full Screen / Esc](#)[Printer-friendly Version](#)[Interactive Discussion](#)

zone, allochthonous inputs of organic and inorganic matter could represent sources and sinks for oxygen, DIC and nutrients that must be considered when interpreting our model results.

4.2 Net production rates

We set 110 m as the mean compensation depth because it is the approximate depth of maxima in the integrated net production and remineralization rates for nitrate and for oxygen at ESTOC (see Fig. 7). DIC and oxygen at BATS actually have maxima at 80–90 m, but they all have inflection points near 110 m, and the 110 m integrals are not greatly different (20% lower for DIC at ESTOC and O₂ at BATS; 2% lower for DIC at BATS). Net production rates and all the integrated model terms, including the associated errors, computed below the mixed layer to 110 m from April to December for both stations, are shown in Table 1 and Fig. 8.

Net production rates computed for oxygen ($1.34 \pm 0.79 \text{ mol O}_2 \text{ m}^{-2}$), dissolved inorganic carbon ($-1.73 \pm 0.52 \text{ mol C m}^{-2}$) and nitrate ($-125 \pm 36 \text{ mmol N m}^{-2}$) at BATS showed no statistically significant differences compared to ESTOC ($1.03 \pm 0.62 \text{ mol O}_2 \text{ m}^{-2}$, $-1.42 \pm 0.30 \text{ mol C m}^{-2}$ and $-213 \pm 56 \text{ mmol N m}^{-2}$). In agreement with previous geochemical estimates (Riser and Johnson, 2008) our results indicate that in these regions, at least for a seasonal scale, photosynthesis exceeds remineralization of organic matter.

The comparison of the observed changes in the tracers inventories and the modelled net production evidences the relevance of the physical fluxes, as the change in the tracers, in general, underestimated biological net production. The change in the tracers inventories underestimated oxygen net production rates by 163% at BATS and 136% at ESTOC. For DIC the underestimation was 63% at ESTOC, whereas it was overestimated by 17% at BATS. For nitrate the underestimation was 97% at BATS and 102% at ESTOC. The contribution of diffusion was larger than total advection (horizontal+vertical) for all the tracers at both stations except DIC at BATS.

BGD

8, 12477–12519, 2011

Regional differences in NP and shallow remineralization

B. Fernández-Castro et al.

Title Page

Abstract

Introduction

Conclusions

References

Tables

Figures

⏪

⏩

◀

▶

Back

Close

Full Screen / Esc

Printer-friendly Version

Interactive Discussion

**Regional differences
in NP and shallow
remineralization**

B. Fernández-Castro et
al.

[Title Page](#)[Abstract](#)[Introduction](#)[Conclusions](#)[References](#)[Tables](#)[Figures](#)[⏪](#)[⏩](#)[◀](#)[▶](#)[Back](#)[Close](#)[Full Screen / Esc](#)[Printer-friendly Version](#)[Interactive Discussion](#)

5 Computed net production rates compared with a summary of previous values reported for BATS and ESTOC are presented in Table 2, where different integration periods must be interpreted carefully. Gruber et al. (1998) and Brix et al. (2006) estimated that net production at BATS during the spring-summer period represents 60–80 % of the total annual net production. Similar results were obtained at ESTOC by González-Dávila et al. (2003). As the integration interval (April–December) used for our estimates misses part of the winter-spring bloom (Brix et al., 2006; González-Dávila et al., 2007, 2010), our rates are probably lower than annual estimates. According to Marchal et al. (1996), net production in the mixed layer in the Sargasso Sea represented 10 60 % of the photic layer net production. Assuming this is true also for ESTOC, our rates would represent about 40 % of the total net production, i.e. $3.4 \text{ mol O}_2 \text{ m}^{-2}$ and $-4.3 \text{ mol C m}^{-2}$ at BATS and $2.6 \text{ mol O}_2 \text{ m}^{-2}$ and $-3.6 \text{ mol C m}^{-2}$ at ESTOC. As nitrate consumption is only observed in the lower photic layer, this extrapolation is not suitable for this tracer. Using an oxygen tracer model, Musgrave et al. (1988) estimated the rate of net production in the photic layer at BATS to be $3-4 \text{ mol O}_2 \text{ m}^{-2} \text{ yr}^{-1}$, very 15 similar to our estimate ($3.4 \text{ mol O}_2 \text{ m}^{-2}$). Our rate for net production of carbon at BATS ($1.73-4.3 \text{ mol C m}^{-2}$) is in the range of previous estimates using mixed layer model approaches ($1.8-4.0 \text{ mol C m}^{-2}$, Marchal et al. (1996); Gruber et al. (1998); Brix et al. (2006)). A compilation of nitrogen inputs carried out in the Sargasso Sea including wet and dry deposition, convective, diapycnal and isopycnal mixing, Ekman transport, mesoscale eddies and nitrogen fixation quantified annual production in $0.37-1.39 \text{ mol N m}^{-2} \text{ yr}^{-1}$ (Lipschultz et al., 2002). Our estimate for net production of nitrogen at BATS ($0.125 \pm 0.036 \text{ mol N m}^{-2}$), which neglects important sources of nitrogen as nitrogen fixation, convective mixing and mesoscale structures, does not reach the 20 lower end of this compilation. Our estimate is also lower than the value obtained by Siegel et al. (1999) ($0.48 \pm 0.12 \text{ mol N m}^{-2} \text{ yr}^{-1}$), who reported a compilation of new nitrogen inputs where nitrogen fixation was not included.

González-Dávila et al. (2003), by using a mixed-layer model for ESTOC that did not include lateral advection, estimated net production of carbon in the mixed layer between 25

April and October, and the period 1996–2001, to be $25.5 \pm 5.7 \text{ mmol C m}^{-3}$. This value corresponds to a mixed layer net production rate of $1.55 \pm 0.75 \text{ mol C m}^{-2}$, computed considering the averaged depth of the mixed layer during this period ($61 \pm 26 \text{ m}$). Following the same approach but using a longer data set (1995–2004), González-Dávila et al. (2007) estimated net production in the mixed layer to be $3.3 \pm 0.8 \text{ mol C m}^{-2}$. Both rates are in close agreement with our estimate ($1.42\text{--}3.6 \text{ mol C m}^{-2}$). Our rate of net production based on nitrate ($0.213 \pm 0.053 \text{ mol N m}^{-2}$) is only slightly lower than the total new nitrogen inputs reported by Cianca et al. (2007) at ESTOC ($0.28 \pm 0.09 \text{ mol N m}^{-2} \text{ yr}^{-1}$), who considered eddy pumping, convective, diapycnal and isopycnal mixing, and Ekman transport.

The $-O_2:C$ ratios computed from the net production estimates at BATS (0.77 ± 0.51) and ESTOC (0.72 ± 0.46) are lower than the ratio for NO_3 -based production (1.4, Gruber (2008)) and closer to the ratio for NH_4 -based production (1.1). The lower $-O_2:C$ ratio at ESTOC could be related to the remineralization peak observed during the fall (September–November), which was more intense for oxygen than for DIC, probably due to the larger lateral inputs (see Fig. 6). When the biological source term at ESTOC was integrated between April and September, excluding the remineralization pulse observed in autumn, the $-O_2:C$ ratio (1.30 ± 0.62) was closer to the standard values. Net production rates computed between April and December with the geostrophic model term set to zero (see Sect. 3.2.1) gave a $-O_2:C$ ratio of ~ 1.0 , also in better agreement with the canonic values. At BATS, we attributed the low $-O_2:C$ ratio to the diffusion simulation that causes a strong oxygen consumption between the mixed-layer depth and 35 m. If this region was not included in the integration, oxygen production rate would be increased ($2.14 \pm 0.37 \text{ mol O}_2 \text{ m}^{-2}$) and DIC production rate lowered ($-1.20 \pm 0.21 \text{ mol C m}^{-2}$), resulting in higher than Redfield ratio (1.78 ± 0.86). The C:N value at BATS (13.9 ± 5.8) was higher than the Redfield ratio (6.6) and very similar at ESTOC (6.7 ± 2.3). However, this fact is slightly deceiving in that most of the oxygen production and DIC uptake occurs above 80 m, while most of the NO_3 uptake occurs between 80–110 m, which is not constant Redfield C:N coupling.

Regional differences in NP and shallow remineralization

B. Fernández-Castro et al.

[Title Page](#)[Abstract](#)[Introduction](#)[Conclusions](#)[References](#)[Tables](#)[Figures](#)[⏪](#)[⏩](#)[◀](#)[▶](#)[Back](#)[Close](#)[Full Screen / Esc](#)[Printer-friendly Version](#)[Interactive Discussion](#)

4.3 Remineralization rates

All the model terms were integrated between April and December and 110–250 m to obtain shallow remineralization rates (see Figure 9 and Table 3). Oxygen ($-1.81 \pm 0.37 \text{ mol O}_2 \text{ m}^{-2}$) and DIC ($1.52 \pm 0.30 \text{ mol C m}^{-2}$) remineralization rates computed for BATS were in good agreement with those reported by Ono et al. (2001) ($-2.08 \pm 0.38 \text{ mol O}_2 \text{ m}^{-2}$ and $-1.53 \pm 0.35 \text{ mol C m}^{-2}$), whereas nitrate remineralization rate ($147 \pm 43 \text{ mmol N m}^{-2}$) was twice the rate reported by these authors ($80 \pm 46 \text{ mmol N m}^{-2}$). This mismatch was due to the differences in the geostrophic lateral advection term ($-51 \pm 44 \text{ mmol N m}^{-2}$ versus $39 \pm 39 \text{ mmol N m}^{-2}$ reported by Ono et al.) that resulted from the use of different climatologies. Changes in the tracers inventories also underestimated shallow remineralization, as they represented 51 %, 45 % and 21 % of remineralization rates computed for oxygen, DIC and nitrate, respectively.

Shallow remineralization rates computed for ESTOC were significantly higher than at BATS for oxygen ($-3.9 \pm 1.0 \text{ mol O}_2 \text{ m}^{-2}$) but showed no significant differences for DIC ($1.53 \pm 0.43 \text{ mol C m}^{-2}$) and nitrate ($38 \pm 155 \text{ mmol N m}^{-2}$). The later was associated with large errors. The change in the tracers inventories underestimated remineralization rates for oxygen and DIC as represented 17 and 36 % of these rates. However, nitrate remineralization rate was overestimated (340 %) by the change in the inventory.

Diffusion was a source for oxygen and a sink for DIC and nitrate in both stations because oxygen (DIC/nitrate) gradient was negative (positive) downwards and greater at 110 m than 250 m. Vertical advection was a source for all the tracers at BATS because w was negative at 110 m and zero at 250 m, whereas it was a sink at ESTOC because upwelling was dominant during the investigation period. Lateral transport (geostrophic horizontal advection) was a source (sink) for oxygen (nitrate/DIC) at BATS and a source (sink) for oxygen and nitrate (DIC) at ESTOC. The lateral transport at ESTOC could explain the differences in the remineralization rates computed for both stations, as the 1-D model without geostrophic advection resulted in oxygen

BGD

8, 12477–12519, 2011

Regional differences in NP and shallow remineralization

B. Fernández-Castro et al.

Title Page

Abstract

Introduction

Conclusions

References

Tables

Figures

⏪

⏩

◀

▶

Back

Close

Full Screen / Esc

Printer-friendly Version

Interactive Discussion

consumption rates reduced by 56 % at ESTOC ($-1.73 \pm 0.30 \text{ mol O}_2 \text{ m}^{-2}$) and only by 16 % at BATS ($-1.18 \pm 0.10 \text{ mol O}_2 \text{ m}^{-2}$).

Remineralization rates computed at BATS were comparable with previous estimates reported in the region (see Table 4). Jenkins and Goldman (1985) calculated the shallow (100–250 m) oxygen consumption rate between April and November at station S in the Sargasso Sea to be $3 \text{ mol O}_2 \text{ m}^{-2}$. Sarmiento et al. (1990) summarized remineralization rates determined from a variety of tracer based techniques in the Sargasso Sea to be $0.6\text{--}3.3 \text{ mol O}_2 \text{ m}^{-2} \text{ yr}^{-1}$. Carlson et al. (1994) estimated the remineralization of dissolved organic matter from spring to fall as $0.99\text{--}1.21 \text{ mol C m}^{-2}$, lower than our estimate as it did not include the particulate organic fraction.

To our knowledge, geochemical estimates of shallow remineralization based on tracer distributions have not been conducted at ESTOC so far. Alonso-González et al. (2009) used a box model approach to calculate the lateral transport and consumption of suspended particulate organic matter (POC) in the Canary Current region. They found that lateral POC fluxes, which were up to 3 orders of magnitude higher than vertical fluxes, accounted for $1.42 \text{ mmol C m}^{-2} \text{ d}^{-1}$, what represents 28–59 % of the total mesopelagic (100–700 m) respiration. The total carbon consumption estimated for mesopelagic waters in the fall was $2.4\text{--}5.1 \text{ mmol C m}^{-2} \text{ d}^{-1}$, slightly lower than our estimate ($6.7 \pm 1.9 \text{ mmol C m}^{-2} \text{ d}^{-1}$) and one order of magnitude lower than respiration rates obtained during the summer by using combined in vitro oxygen consumption and enzymatic activity techniques ($68 \text{ mmol C m}^{-2} \text{ d}^{-1}$) in the subtropical Northeast Atlantic (Aristegui et al., 2005). Alonso-González et al. hypothesized that this mismatch could be due to the different times of the year when the experiments were carried out. However, recent studies indicate that long incubations may lead to overestimations of community respiration as a result of an increase in the activity of heterotrophic bacteria (Marañón et al., 2007; Calvo-Díaz et al., 2011). Due to the differences in integration depths, comparison with these studies must be done carefully.

Shallow remineralization rates computed by our model can also be compared to particulate organic matter attenuation flux computed from sediment traps deployed

BGD

8, 12477–12519, 2011

Regional differences in NP and shallow remineralization

B. Fernández-Castro et al.

Title Page

Abstract

Introduction

Conclusions

References

Tables

Figures

⏪

⏩

◀

▶

Back

Close

Full Screen / Esc

Printer-friendly Version

Interactive Discussion



at BATS and ESTOC. Comparative information for sediment traps for both stations corresponds to 150, 200 and 300 m at BATS and 200, 300 and 500 m at ESTOC (Helmke et al., 2010). In order to estimate remineralization rates between 110 and 250 m the particle flux at 110 and 250 m needs to be inferred. The former was calculated using the Martin's attenuation equation (Martin et al., 1987), considering the seasonal b exponents calculated by Helmke et al. (2010) ($b = 0.6\text{--}1.19$) for BATS, and the value reported by Neuer et al. (2007) ($b = 0.81$) for ESTOC. The particulate flux at 250 m was calculated by linearly interpolating the flux measured at 200 and 300 m. Shallow remineralization computed from springtime to fall was $0.38 \text{ mol C m}^{-2}$ at BATS and $0.08 \text{ mol C m}^{-2}$ at ESTOC. Both values were lower than our estimates, which included the dissolved and particulate organic fractions, and represented 25 and 5% of the carbon remineralization computed for BATS and ESTOC, respectively. The sum of the remineralization rates of particulate and dissolved organic matter at BATS ($1.37\text{--}1.59 \text{ mol C m}^{-2}$) matches our estimation of carbon remineralization ($1.52 \pm 0.30 \text{ mol C m}^{-2}$). Unfortunately, no information about the seasonal variability of the dissolved organic carbon cycle is available at ESTOC.

Our results indicated that lateral transport is significant to the seasonality of the hydrodynamic conditions and the tracer distribution at ESTOC. Previous studies indicated that higher remineralization in the subtropical Northeast Atlantic could be supported by dissolved (Álvarez-Salgado et al., 2007) and slow sinking particulate organic matter (Alonso-González et al., 2009) exported from the high productive African coastal upwelling, and also by dark dissolved inorganic carbon fixation (Baltar et al., 2010). In this respect, Arístegui et al. (2003) estimated that the contribution of dissolved organic carbon to the mesopelagic oxygen consumption in the Canary Current region was about 30%. Due to the relevance of the allochthonous sources of organic matter at ESTOC, we cannot assert that the differences in shallow remineralization computed for both stations could explain a significant fraction of the observed discrepancy in carbon export rates. Alonso-González et al. (2009) indicated that this difference could be, at least partially, explained by low sedimentation rates of the particulate organic matter

Regional differences in NP and shallow remineralization

B. Fernández-Castro et al.

[Title Page](#)[Abstract](#)[Introduction](#)[Conclusions](#)[References](#)[Tables](#)[Figures](#)[⏪](#)[⏩](#)[◀](#)[▶](#)[Back](#)[Close](#)[Full Screen / Esc](#)[Printer-friendly Version](#)[Interactive Discussion](#)

in the eastern part, as slow-sinking or suspended POC does not accumulate in the sediment traps and can be laterally advected (Aristegui et al., 2009).

According to our results shallow remineralization represents at BATS $54 \pm 33\%$ and $51 \pm 36\%$ of the net production computed in the photic zone for oxygen and DIC, respectively, whereas at ESTOC it represents $151 \pm 99\%$ and $43 \pm 15\%$ respectively. The high value for oxygen at ESTOC is related to the strong lateral inputs computed in the fall (see oxygen geostrophic horizontal advection in Fig. 6), that also resulted in negative net production computed during these months (see oxygen biological source in Fig. 6), suggesting that high remineralization rates could partially be sustained by non-locally produced organic matter.

The $-O_2:C$ ratio for the shallow remineralization computed at BATS (1.19 ± 0.34) was in good agreement with the Redfield ratio (1.43), whereas at ESTOC (2.52 ± 0.98) was slightly higher. C:N ratios were in excess of the Redfield ratio at both stations, and were higher at ESTOC (40 ± 162) than at BATS (10.2 ± 3.6), pointing to the export of carbon enriched organic matter. The C:N ratio reported by Ono et al. (2001) for BATS (19 ± 12) was twice our estimate, as a consequence of the differences in nitrate remineralization estimates. The higher C:N ratio computed for ESTOC was consistent with the carbon rich organic matter observed in the mixed layer (Koeve, 2006) and the sinking organic matter (Neuer et al., 2007) in the region, and with close to Redfield ratios observed in the sinking organic matter at BATS (Schnetzer and Steinberg, 2002). Moreover, ecological models employed to study the sensitivity of carbon export to atmospheric nitrogen inputs in NASW and NASE showed higher C:N values in the sinking organic matter in NASE (Mouriño-Carballido et al., 2011, under revision).

5 Conclusions

Subtropical gyres play a crucial role in the global carbon cycle due to the large extension they occupy which is expected to get large as a consequence of global warming (Polovina et al., 2008). Understanding the heterogeneity of these biomes is critical to

Regional differences in NP and shallow remineralization

B. Fernández-Castro et al.

Title Page

Abstract

Introduction

Conclusions

References

Tables

Figures

⏪

⏩

◀

▶

Back

Close

Full Screen / Esc

Printer-friendly Version

Interactive Discussion



**Regional differences
in NP and shallow
remineralization**B. Fernández-Castro et
al.

[Title Page](#)[Abstract](#)[Introduction](#)[Conclusions](#)[References](#)[Tables](#)[Figures](#)[Back](#)[Close](#)[Full Screen / Esc](#)[Printer-friendly Version](#)[Interactive Discussion](#)

comprehend the role of the oceans in the future carbon cycle. By using a 1-D diagnostic tracer model we investigated if potential differences in net production and shallow remineralization could explain the lower export of particulate organic carbon observed at the eastern (ESTOC) compared to the western side (BATS) of the North Atlantic Subtropical gyre. Our results showed that net production was not statistically different at both stations, whereas oxygen shallow remineralization was higher at ESTOC. As our approach misses part of the winter-spring bloom period, we can not discard that it underestimates the differences in net production between the two stations. Our results are consistent with enhanced respiration processes at ESTOC. However, the importance of horizontal processes in the seasonal cycles at ESTOC indicates that oxygen consumption at this station could be also supported by allochthonous inputs of organic matter. The comparison of our estimates with vertical fluxes of POC shows that whereas a significant fraction (25 %) of the shallow remineralization is sustained by sinking organic matter at BATS, this fraction is much lower at ESTOC (5 %). There is still work to be done to fully understand the mechanisms behind the regional differences observed in the vertical export of carbon at the North Atlantic subtropical gyre. At the light of this and other studies it seems that crucial information must come from the study of horizontal fluxes at ESTOC.

Acknowledgements. We are grateful to all the technicians and crew members involved in the collection, preparation, and analysis of the large data sets used in this study, in particular those from the BATS and ESTOC programs. B. Mouriño was supported by the Ramón y Cajal program from the Spanish Minister of Science and Technology. Funding for this study was provided by the Xunta de Galicia under the research project VARITROP (09MDS001312PR, PI B. Mouriño) and by the Ministerio de Ciencia e Innovation MOMAC project (CTM2008-05914/MAR).

References

- Alonso-González, I. J., Arístegui, J., Vilas, J. C., and Hernández-Guerra, A.: Lateral POC transport and consumption in surface and deep waters of the Canary Current region: A box model study, *Global Biogeochem. Cy.*, 23, GB2007, doi:10.1029/2008GB003185, 2009. 12492, 12497, 12498, 12510
- Álvarez-Salgado, X. A., Arístegui, J., Barton, E. D., and Hansell, D. A.: Contribution of upwelling filaments to offshore carbon export in the subtropical Northeast Atlantic Ocean, *Limnol. Oceanogr.*, 52, 1287–1292, 2007. 12480, 12498
- Antonov, J. I., Seidov, D., Boyer, T. P., Locarni, R. A., Mishonov, A. V., Garcia, H. E., Baranova, O. K., Zweng, M. M., and Johnson, D. R.: *World Ocean Atlas 2009, Volume 2: Salinity.*, Ed. NOAA Atlas NESDIS 69, U.S. Government Printing Office, Washington, D.C., 2010. 12487
- Arístegui, J., Barton, E., Montero, M., García-Muñoz, M., and Escánez, J.: Organic carbon distribution and water column respiration in the NW Africa-Canaries Coastal Transition Zone, *Aquat. Microb. Ecol.*, 33, 289–301, 2003. 12492, 12498, 12510
- Arístegui, J., Duarte, C. M., Gasol, J. M., and Alonso-Sáez, L.: Active mesopelagic prokaryotes support high respiration in the subtropical northeast Atlantic Ocean, *Geophys. Res. Lett.*, 32, L03608, doi:10.1029/2008GB003185, 2005. 12497, 12510
- Arístegui, J., Gasol, J. M., Duarte, C. M., and Herndl, G. J.: Microbial oceanography of the dark ocean's pelagic realm, *Limnol. Oceanogr.*, 54, 1501–1529, doi:10.4319/lo.2009.54.5.1501, 2009. 12499
- Baltar, F., Arístegui, J., Sintés, E., Gasol, J. M., Reinthaler, T., and Herndl, G. J.: Significance of non-sinking particulate organic carbon and dark CO₂ fixation to heterotrophic carbon demand in the mesopelagic northeast Atlantic, *Geophys. Res. Lett.*, 37, L09602, doi:10.1029/2010GL043105, 2010. 12498
- Bonnet, S., Grosso, O., and Moutin, T.: Planktonic dinitrogen fixation along a longitudinal gradient across the Mediterranean Sea during the stratified period (BOUM cruise), *Biogeosciences*, 8, 2257–2267, doi:10.5194/bg-8-2257-2011, 2011. 12481
- Brix, H., Gruber, N., Karl, D. M., and Bates, N. R.: On the relationships between primary, net community, and export production in subtropical gyres, *Deep Sea. Res. Pt. II*, 53, 698–717, 2006. 12494, 12508
- Calvo-Díaz, A., Díaz-Pérez, L., G Morán, X. A., Teira, E., and Marañón, E.: Bottle enclosure causes a decrease in the autotrophic to heterotrophic biomass ratio of picoplankton in olig-

Regional differences in NP and shallow remineralization

B. Fernández-Castro et al.

Title Page

Abstract

Introduction

Conclusions

References

Tables

Figures

⏪

⏩

◀

▶

Back

Close

Full Screen / Esc

Printer-friendly Version

Interactive Discussion



Regional differences in NP and shallow reminerzalization

B. Fernández-Castro et
al.

Title Page

Abstract

Introduction

Conclusions

References

Tables

Figures

⏪

⏩

◀

▶

Back

Close

Full Screen / Esc

Printer-friendly Version

Interactive Discussion



and 2000, *Global Biogeochem. Cy.*, 17, 1076, doi:10.1029/2002GB001993, 2003. 12484, 12485, 12494, 12508

González-Dávila, M., Santana-Casiano, J. M., and González-Dávila, E. F.: Interannual variability of the upper ocean carbon cycle in the northeast Atlantic Ocean, *Geophys. Res. Lett.*, 34, L07608, doi:10.1029/2006GL028145, 2007. 12494, 12495, 12508

González-Dávila, M., Santana-Casiano, J. M., Rueda, M. J., and Llinás, O.: The water column distribution of carbonate system variables at the ESTOC site from 1995 to 2004, *Biogeochemistry*, 7, 3067–3081, doi:10.5194/bg-7-3067-2010, 2010. 12494

Goyet, C., Healy, R., and Ryan, J.: Global distribution of total inorganic carbon and total alkalinity below the deepest winter mixed layer depths, Environmental Sciences Division, U.S. Department of Energy, 2000. 12487

Gruber, N.: Nitrogen in the Marine Environment, chap. The marine nitrogen cycle: overview and challenges, 1–50, Academic Press, Elsevier Inc., Amsterdam., 2008. 12495

Gruber, N., Keeling, C. D., and Stocker, T. F.: Carbon-13 constraints on the seasonal inorganic carbon budget at the BATS site in the northwestern Sargasso Sea, *Deep-Sea Res. Pt. I*, 45, 673–717, 1998. 12484, 12494, 12508

Helmke, P., Neuer, S., Lomas, M. W., Conte, M., and Freudenthal, T.: Cross-basin differences in particulate organic carbon export and flux attenuation in the subtropical North Atlantic gyre, *Deep-Sea Res. Pt. I*, 57, 213–227, doi:10.1016/j.dsr.2009.11.001, 2010. 12481, 12498, 12510

Jenkins, W. and Goldman, J.: Seasonal oxygen cycling and primary production in the Sargasso Sea, *J. Mar. Res.*, 43, 465–491, 1985. 12485, 12497, 12510

Koeve, W.: C:N stoichiometry of the biological pump in the North Atlantic: Constraints from climatological data, *Global Biogeochem. Cy.*, 20, GB3018, doi:10.1029/2004GB002407, 2006. 12499

Leetmaa, A. and Bunker, A. F.: Updated charts of the mean annual wind stress, convergences in Ekman Layers, and Sverdrup transport in the North Atlantic, *J. Mar. Res.*, 36, 311–322, 1978. 12488

Lipschultz, F., Bates, N., Carlson, C., and Hansell, D.: New production in the Sargasso Sea: History and current status, *Global Biogeochem. Cy.*, 16, 1001, 2002. 12494, 12508

Locarnini, R. A., Mishonov, A. V., Antonov, J. I., Boyer, T., Garcia, H., Baranova, O. K., Zweng, M. M., and Johnson, D. R.: *World Ocean Atlas 2009, Volume 1: Temperature*, NOAA Atlas NESDIS 68, U.S. Government Printing Office, Washington, D.C., 2010. 12487

Regional differences in NP and shallow reminerzalization

B. Fernández-Castro et
al.

Title Page

Abstract

Introduction

Conclusions

References

Tables

Figures

◀

▶

◀

▶

Back

Close

Full Screen / Esc

Printer-friendly Version

Interactive Discussion

- circulation and offshore pumping of organic matter, *J. Mar. Syst.*, 54, 3–37, 2005. 12480, 12487, 12492
- Polovina, J. J., Howell, E. A., and Abecassis, M.: Ocean's least productive waters are expanding, *Geophys. Res. Lett.*, 35, L03618, <http://dx.doi.org/10.1029/2007GL031745>, 2008. 12499
- 5 Pulido-Villena, E., Wagener, T., and Guieu, C.: Bacterial response to dust pulses in the western Mediterranean: Implications for carbon cycling in the oligotrophic ocean, *Global Biochem. Cy.*, 22, GB1020, doi:10.1029/2007GB003091, 2008. 12481
- Riser, S. C. and Johnson, K. S.: Net production of oxygen in the subtropical ocean, *Nature*, 451, 323–U5, doi:10.1038/nature06441, 2008. 12493
- 10 Santana-Casiano, J. M., González-Dávila, M., Rueda, M.-J., Llinás, O., and González-Dávila, E.-F.: The interannual variability of oceanic CO₂ parameters in the northeast Atlantic subtropical gyre at the ESTOC site, *Global Biogeochem. Cy.*, 21, GB1015, doi:10.1029/2006GB002788, 2007. 12485
- Sarmiento, J., Thiele, G., Key, R., and Moore, W.: Oxygen and nitrate new production and remineralization in the North-Atlantic Subtropical Gyre, *J. Geophys. Res.-Ocean*, 95, 18303–18315, 1990. 12497, 12510
- 15 Schnetzer, A. and Steinberg, D. K.: Active transport of particulate organic carbon and nitrogen by vertically migrating zooplankton in the Sargasso Sea, *Mar. Ecol.-Prog. Ser.*, 234, 71–84, doi:10.3354/meps234071, 2002. 12499
- 20 Siegel, D. A. and Deuser, W. G.: Trajectories of sinking particles in the Sargasso Sea: modeling of statistical funnels above deep-ocean sediment traps, *Deep-Sea Res. Pt. I*, 44, 1519–1541, 1997. 12487
- Siegel, D. A., McGillicuddy, D. J., and Fields, E. A.: Mesoscale eddies, satellite altimetry, and new production in the Sargasso Sea, *J. Geophys. Res.*, 104, 13359–13379, 1999. 12481, 12494, 12508
- 25 Steinberg, D. K., Carlson, C. A., Bates, N. R., Johnson, R. J., Michaels, A. F., and Knap, A. H.: Overview of the US JGOFS Bermuda Atlantic Time-series Study (BATS): a decade-scale look at ocean biology and biogeochemistry, *Deep-Sea Res. Pt. II*, 48, 1405–1447, 2001. 12480

Regional differences in NP and shallow remineralization

B. Fernández-Castro et al.

Table 1. Integrated model terms computed from the mixed layer depth to 110 m, and from April to December. The geostrophic horizontal advection term (see Sect. 3.2.1) is also included in the table.

	BATS			ESTOC		
	O ₂ (mol m ⁻²)	DIC (mol m ⁻²)	NO ₃ (mmol m ⁻²)	O ₂ (mol m ⁻²)	DIC (mol m ⁻²)	NO ₃ (mmol m ⁻²)
Net Production	1.34 ± 0.79	-1.73 ± 0.52	-125 ± 36	1.03 ± 0.62	-1.42 ± 0.30	-213 ± 56
Budget change	-0.850 ± 0.075	-2.03 ± 0.16	-24 ± 21	-0.372 ± 0.074	-0.518 ± 0.062	5.4 ± 4.8
Diffusion	-1.81 ± 0.60	-0.24 ± 0.30	80 ± 19	-2.32 ± 0.45	0.69 ± 0.19	171 ± 26
Vertical advection	1.39 ± 0.27	12.9 ± 2.5	-7.4 ± 1.2	-0.160 ± 0.056	-1.43 ± 0.50	0.42 ± 0.52
Total hor. adv.	-1.77 ± 0.46	-13.0 ± 2.5	28 ± 17	1.08 ± 0.40	1.65 ± 0.55	47 ± 44
Geostrophic hor. adv.	-0.32 ± 0.18	0.00 ± 0.12	27.4 ± 7.9	0.95 ± 0.48	-0.13 ± 0.22	44 ± 47

[Title Page](#)
[Abstract](#)
[Introduction](#)
[Conclusions](#)
[References](#)
[Tables](#)
[Figures](#)
[Back](#)
[Close](#)
[Full Screen / Esc](#)
[Printer-friendly Version](#)
[Interactive Discussion](#)

Regional differences in NP and shallow remineralization

B. Fernández-Castro et al.

Table 3. Integrated model terms computed from 110 m down to 250 m, and from April to December. The geostrophic horizontal advection term (see Sect. 3.2.1) is also included in the table.

	O_2 (mol m ⁻²)	BATS DIC (mol m ⁻²)	NO_3 (mmol m ⁻²)	O_2 (mol m ⁻²)	ESTOC DIC (mol m ⁻²)	NO_3 (mmol m ⁻²)
Remineralization	-1.81 ± 0.37	1.52 ± 0.30	147 ± 43	-3.9 ± 1.0	1.53 ± 0.43	38 ± 155
Budget change	-0.93 ± 0.17	0.69 ± 0.24	32 ± 25	-0.68 ± 0.20	0.55 ± 0.15	130 ± 21
Diffusion	0.44 ± 0.23	-0.64 ± 0.23	-60 ± 21	1.49 ± 0.33	-0.94 ± 0.22	-13 ± 26
Vertical advection	2.63 ± 0.48	25.6 ± 4.7	7.1 ± 1.4	-0.25 ± 0.11	-2.3 ± 1.0	-0.39 ± 0.54
Total Hor. adv.	-2.19 ± 0.62	-25.8 ± 4.7	-62 ± 39	1.95 ± 0.98	2.3 ± 1.2	105 ± 151
Geostrophic hor. adv.	-0.39 ± 0.33	-0.82 ± 0.30	-51 ± 44	1.9 ± 1.4	-0.80 ± 0.90	84 ± 197

Title Page

Abstract

Introduction

Conclusions

References

Tables

Figures

⏪

⏩

◀

▶

Back

Close

Full Screen / Esc

Printer-friendly Version

Interactive Discussion

Regional differences
in NP and shallow
reminerizationB. Fernández-Castro et
al.

Title Page

Abstract

Introduction

Conclusions

References

Tables

Figures

◀

▶

◀

▶

Back

Close

Full Screen / Esc

Printer-friendly Version

Interactive Discussion



Table 4. Summary for remineralization estimates at BATS and ESTOC. AOU is apparent oxygen utilization; DOC, dissolved organic carbon; POC, particulate organic carbon; ETS, electron transport system and OC is organic carbon.

Region	Source	Technique	Period	Depths m	Estimate mol m ⁻²
Sargasso Sea	Jenkins and Goldman (1985)	AOU seasonal cycle	Apr–Nov	100–250	3.0 (O ₂)
Sargasso Sea	Sarmiento et al. (1990)	Tracer Distribution	Annual	100–250	0.6–3.3 (O ₂)
BATS	Carlson et al. (1994)	DOC changes	Apr–Nov	100–250	0.99–1.21 (C)
BATS	from Helmke et al. (2010)	POC Fluxes	Spring–Fall	110–250	0.38 (C)
BATS	Ono et al. (2001)	Tracer Model	Apr–Dec	100–250	2.08 ± 0.38 (O ₂)
				100–250	1.53 ± 0.35 (C)
				100–250	0.080 ± 0.046 (N)
BATS	This study	Tracer Model	Apr–Dec	110–250	1.81 ± 0.37 (O ₂)
					1.52 ± 0.30 (C)
					0.147 ± 0.043 (N)
ESTOC	from Helmke et al. (2010)	POC fluxes	Spring–Fall	110–250	0.08 (C)
ESTOC	This Study	Tracer Model	Apr–Dec	110–250	3.9 ± 1.0 (O ₂)
					1.53 ± 0.43 (C)
					0.04 ± 0.16 (N)
					mmol m ⁻² d ⁻¹
Canary Current	Aristegui et al. (2003)	ETS Activity	August	200–1000	7 (C)
Canary Current	Aristegui et al. (2005)	ETS/O ₂ <i>in vitro</i>	Summer	200–1000	68 (C)
Canary Current	Alonso-González et al. (2009)	OC balance	Fall	100–700	2.4–5.1 (C)

Regional differences in NP and shallow remineralization

B. Fernández-Castro et al.

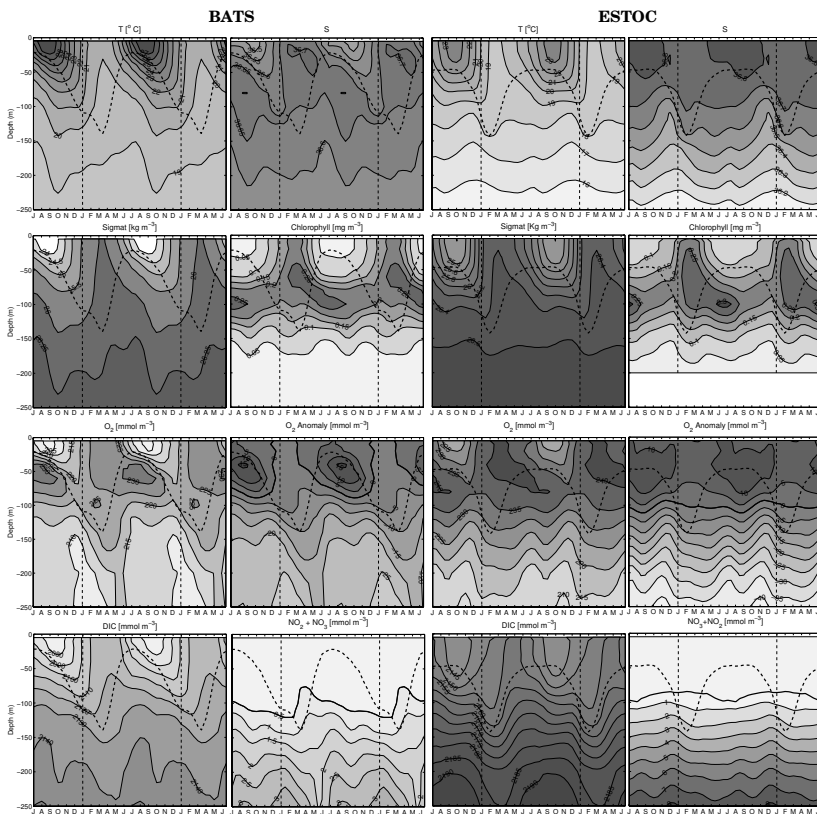


Fig. 1. Seasonal cycles of the vertical distribution of temperature ($^{\circ}\text{C}$), salinity (psu), density anomaly σ_T (kg m^{-3}), chlorophyll a (mg m^{-3}), nitrate + nitrite (mmol m^{-3}), oxygen (mmol m^{-3}), oxygen anomaly (mmol m^{-3}) and dissolved inorganic carbon (DIC) (mmol m^{-3}). Black discontinuous line represents the mixed layer depth. Black thick line represents the isoline of zero oxygen anomaly and the nitracline ($[\text{NO}_3] = 0.5 \text{ mmol m}^{-3}$).

[Title Page](#)
[Abstract](#)
[Introduction](#)
[Conclusions](#)
[References](#)
[Tables](#)
[Figures](#)
[◀](#)
[▶](#)
[◀](#)
[▶](#)
[Back](#)
[Close](#)
[Full Screen / Esc](#)
[Printer-friendly Version](#)
[Interactive Discussion](#)

Regional differences in NP and shallow remineralization

B. Fernández-Castro et al.

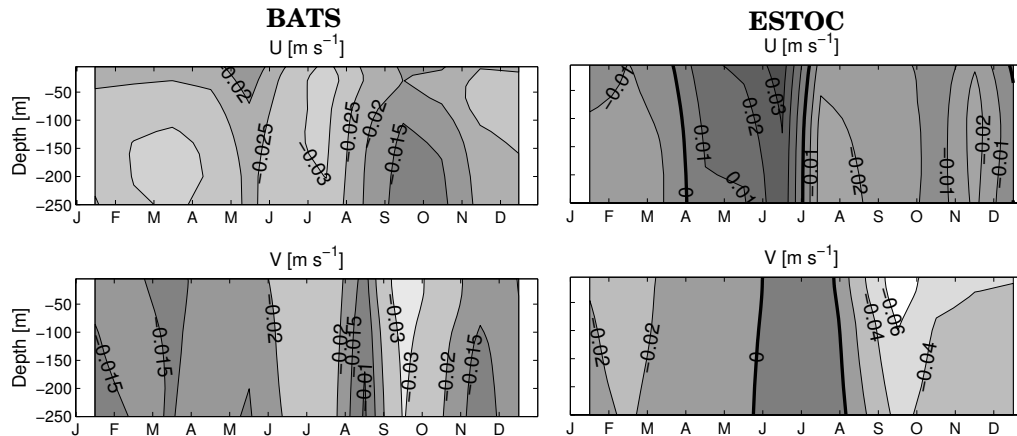


Fig. 2. Computed geostrophic horizontal velocities (u , v) for BATS and ESTOC. The thick black line represents the null velocity component.

Title Page

Abstract

Introduction

Conclusions

References

Tables

Figures



Back

Close

Full Screen / Esc

Printer-friendly Version

Interactive Discussion

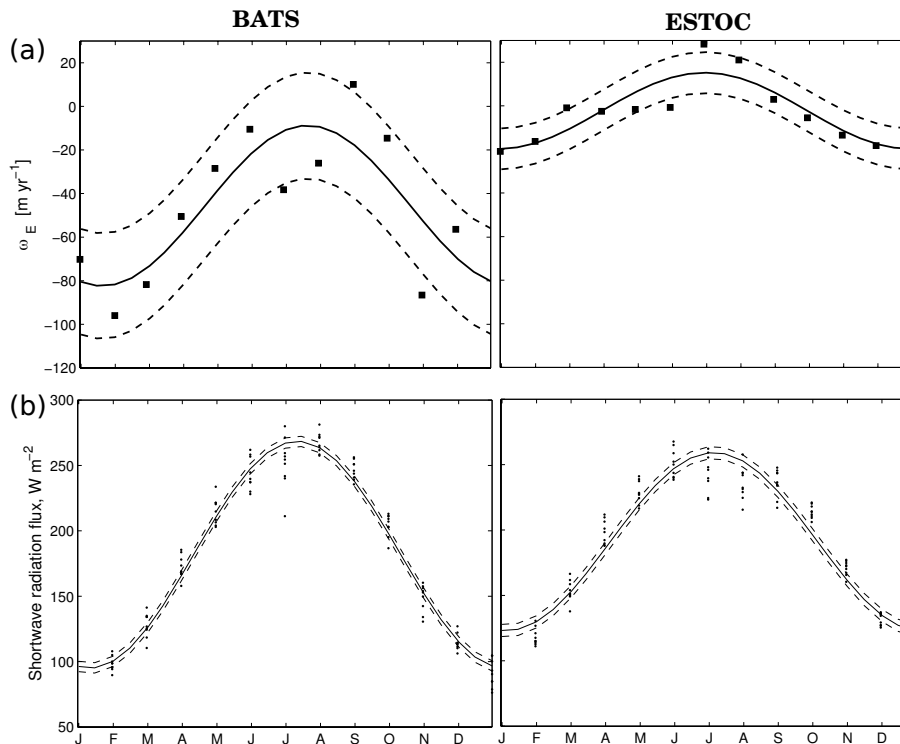
Regional differences
in NP and shallow
reminerzalizationB. Fernández-Castro et
al.

Fig. 3. (a) Vertical Ekman velocity at the Ekman depth (w_E) and (b) surface shortwave solar radiation computed for the period 1996–2001 near BATS and ESTOC. The continuous lines represent the fit to a single harmonic function, whereas the dotted line correspond to the 95% confidence intervals. Fitting of w_E to the harmonic function was not used in the model.

Title Page

Abstract

Introduction

Conclusions

References

Tables

Figures

◀

▶

◀

▶

Back

Close

Full Screen / Esc

Printer-friendly Version

Interactive Discussion

Regional differences in NP and shallow remineralization

B. Fernández-Castro et al.

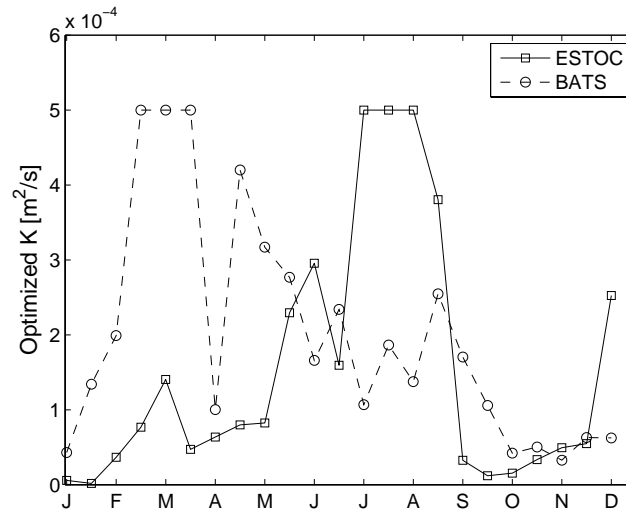


Fig. 4. Optimized diffusivity (K) computed for BATS and ESTOC. Values higher than $5 \text{ cm}^2 \text{ s}^{-1}$ were set to $5 \text{ cm}^2 \text{ s}^{-1}$ on account of numerical limitations in the biological source term calculations.

Title Page

Abstract

Introduction

Conclusions

References

Tables

Figures

◀

▶

◀

▶

Back

Close

Full Screen / Esc

Printer-friendly Version

Interactive Discussion

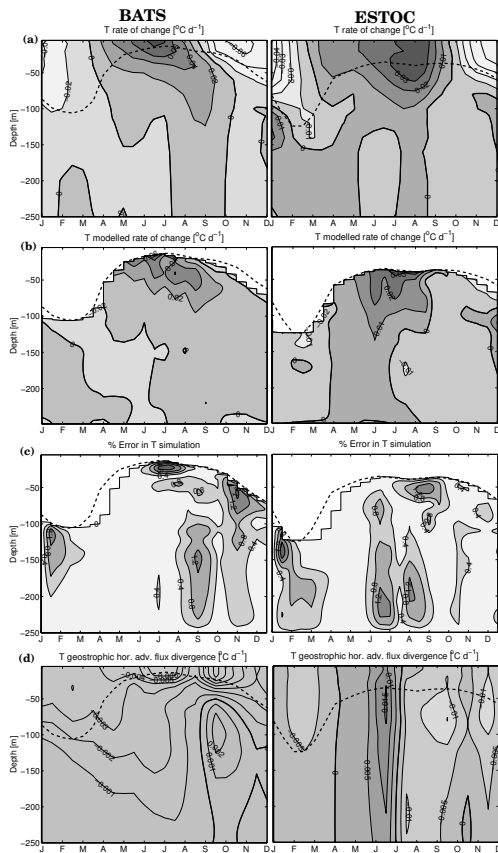


Fig. 5. (a) Observed and (b) simulated temperature rate of change, (c) errors in the simulated temperature seasonal cycle, and (d) contribution of geostrophic horizontal advection to the temperature rate of change at BATS and ESTOC. The black discontinuous line represents the mixed layer depth and the black thick line represents the zero rate of change isoline.

Regional differences in NP and shallow remineralization

B. Fernández-Castro et al.

Title Page

Abstract

Introduction

Conclusions

References

Tables

Figures



Back

Close

Full Screen / Esc

Printer-friendly Version

Interactive Discussion

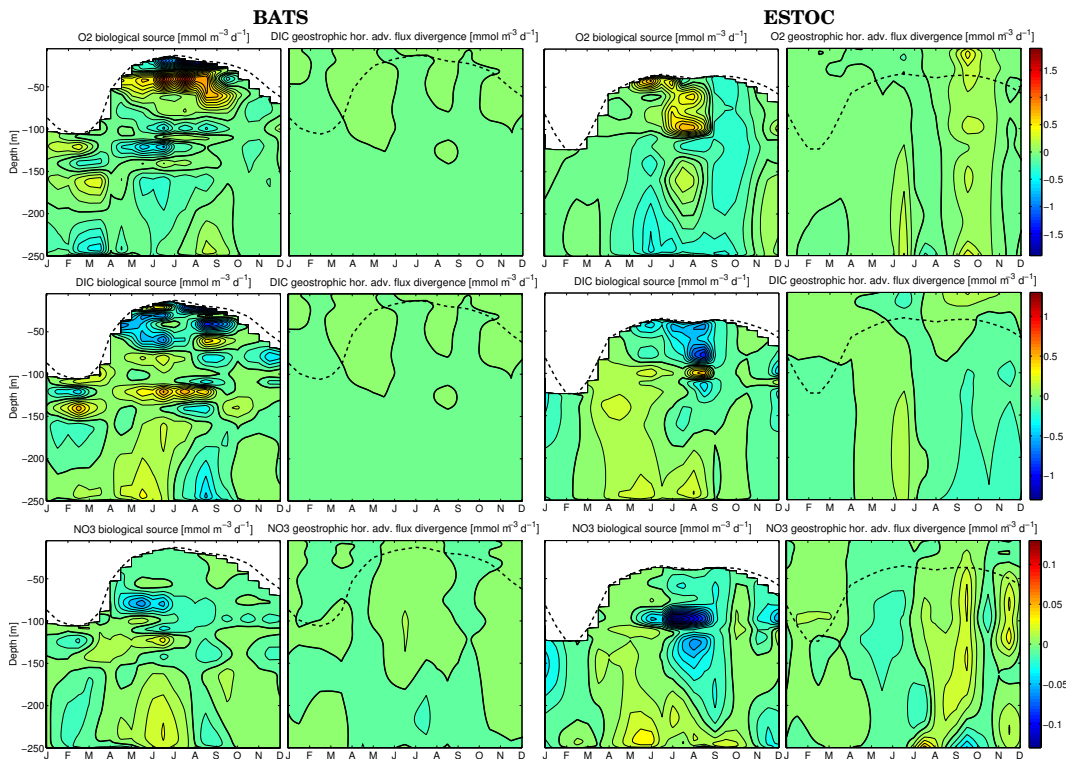
Regional differences
in NP and shallow
reminerzalizationB. Fernández-Castro et
al.

Fig. 6. Biological source term (J_C) and geostrophic horizontal advection flux divergence computed for oxygen, DIC and nitrate at BATS and ESTOC. The discontinuous line represents the mixed-layer depth and the black thick line the zero isoline. Isoline separations are $0.1 \text{ mmol O}_2 \text{ m}^{-3} \text{ d}^{-1}$, $0.1 \text{ mmol C m}^{-3} \text{ d}^{-1}$ and $0.01 \text{ mmol N m}^{-3} \text{ d}^{-1}$, for oxygen, DIC and nitrate, respectively.

Title Page

Abstract

Introduction

Conclusions

References

Tables

Figures

◀

▶

◀

▶

Back

Close

Full Screen / Esc

Printer-friendly Version

Interactive Discussion

Regional differences in NP and shallow remineralization

B. Fernández-Castro et al.

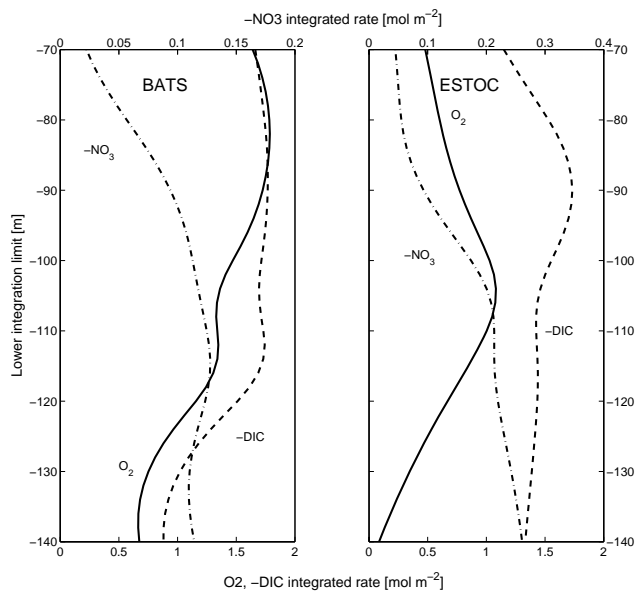


Fig. 7. Time and depth-integrated net production rates as a function of the lower limit used for the integration at BATS and ESTOC for oxygen (solid), DIC (dashed) and nitrate (dot-dashed).

Title Page

Abstract

Introduction

Conclusions

References

Tables

Figures

⏪

⏩

◀

▶

Back

Close

Full Screen / Esc

Printer-friendly Version

Interactive Discussion

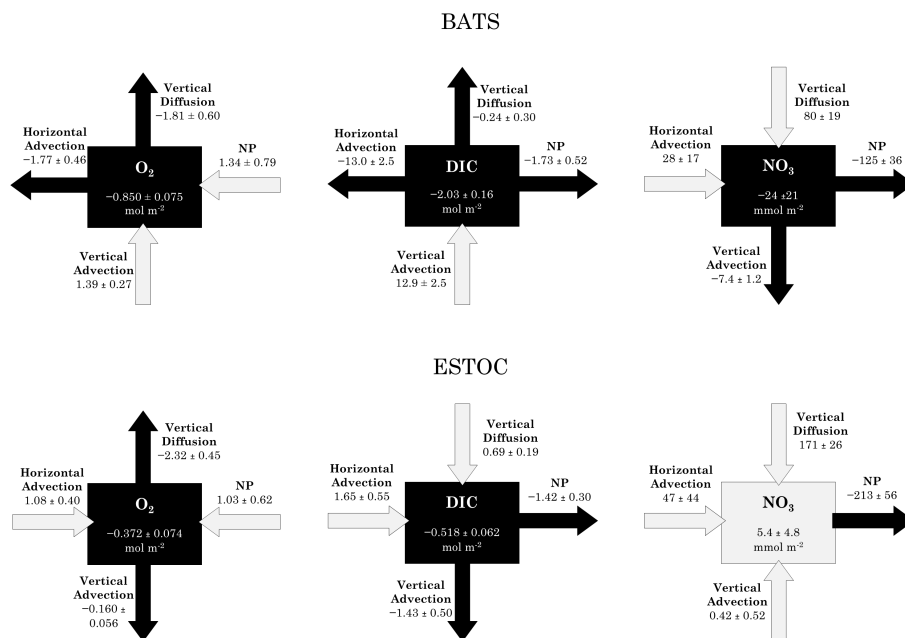
Regional differences
in NP and shallow
reminerzalizationB. Fernández-Castro et
al.

Fig. 8. Integrated model terms computed from the mixed layer depth to 110 m, and from April to December. NP is net production. The white (black) arrows and boxes represent net gain (lost). Rates are expressed in mol m⁻² for oxygen and DIC and in mmol m⁻² for nitrate.

Title Page

Abstract

Introduction

Conclusions

References

Tables

Figures

◀

▶

◀

▶

Back

Close

Full Screen / Esc

Printer-friendly Version

Interactive Discussion

Regional differences in NP and shallow reminerzalization

B. Fernández-Castro et
al.

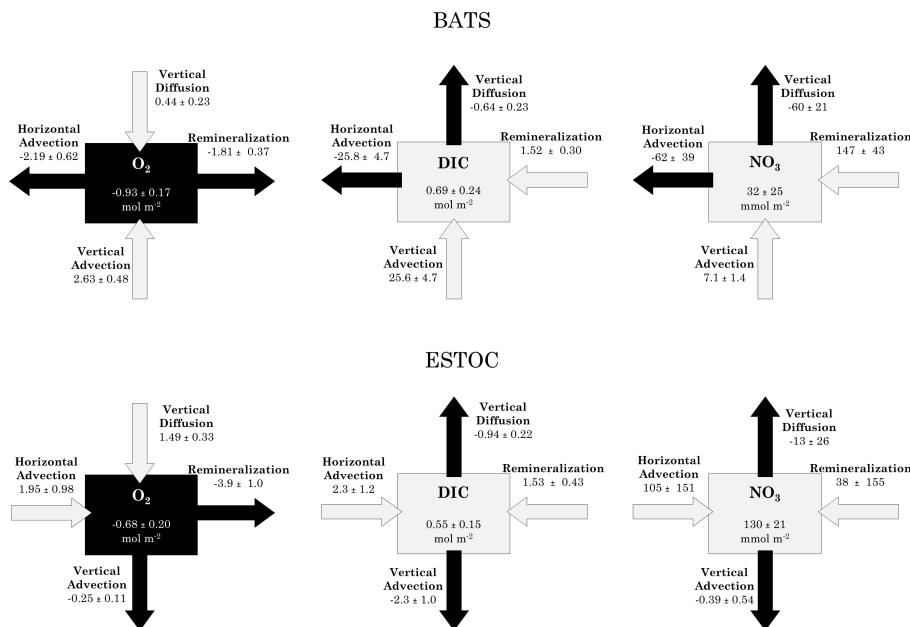


Fig. 9. Integrated model terms computed from 110 m down to 250 m, and from April to December. White (black) arrows and boxed represent net gain (lost). Rates are expressed in mol m⁻² for oxygen and DIC and in mmol m⁻² for nitrate.

[Title Page](#)
[Abstract](#)
[Introduction](#)
[Conclusions](#)
[References](#)
[Tables](#)
[Figures](#)
[⏪](#)
[⏩](#)
[◀](#)
[▶](#)
[Back](#)
[Close](#)
[Full Screen / Esc](#)
[Printer-friendly Version](#)
[Interactive Discussion](#)